Editors' Suggestion

Control-oriented model of dielectrophoresis and electrorotation for arbitrarily shaped objects

Tomáš Michálek,[1,*] Aude Bolopion,[2,†] Zdeněk Hurák,[1] and Michaël Gauthier[2]
[1]*Faculty of Electrical Engineering, Department of Control Engineering, Czech Technical University in Prague, Karlovo náměstí 13, 121 35, Prague, Czech Republic*
[2]*FEMTO-ST Institute, AS2M department Univ. Bourgogne Franche-Comté, CNRS, 24 rue Savary, F-25000 Besançon, France*

(Received 29 November 2018; published 24 May 2019)

The most popular modeling approach for dielectrophoresis (DEP) is the effective multipole (EM) method. It approximates the polarization-induced charge distribution in an object of interest by a set of multipolar moments. The Coulombic interaction of these moments with the external polarizing electric field then gives the DEP force and torque acting on the object. The multipolar moments for objects placed in arbitrary harmonic electric fields are, however, known only for spherical objects. This shape restriction significantly limits the use of the EM method. We present an approach for online (in real time) computation of multipolar moments for objects of arbitrary shapes having even arbitrary internal composition (inhomogeneous objects, more different materials, etc.). We exploit orthonormality of spherical harmonics to extract the multipolar moments from a numerical simulation of the polarized object. This can be done in advance (offline) for a set of external electric fields forming a basis so that the superposition principle can then be used for online operation. DEP force and torque can thus be computed in fractions of a second, which is needed, for example, in model-based control applications. We validate the proposed model against reference numerical solutions obtained using Maxwell stress tensor. We also analyze the importance of the higher-order multipolar moments using a sample case of a Tetris-shaped micro-object placed inside a quadrupolar microelectrode array and exposed to electrorotation. The implementation of the model in MATLAB and COMSOL is offered for free download.

DOI: 10.1103/PhysRevE.99.053307

I. INTRODUCTION

Electrokinetic effects, when exploited at microscale, constitute a fundamental principle of numerous noncontact micromanipulation devices. They use the electric field to impart forces and torques either directly on the objects of interest or indirectly on the liquid medium surrounding them, which then induces a fluid flow carrying the objects to the desired locations.

A widespread representative of the former is the *dielectrophoresis* (DEP). First described by Pohl [1], it is a physical phenomenon enabling actuation of electrically neutral objects. By placing them in an external electric field, they polarize, and the newly emerged charge distribution inside them interacts via Coulomb forces with the source field. In case of an inhomogeneous field, this results in a net force making the object move. Alternating electric fields are commonly used to eliminate the (unwanted) phenomena of *electrolysis* and *electrophoresis* (interaction between the external field and an intrinsic charge potentially present inside the object). Two significant modes of dielectrophoresis are distinguished: *conventional DEP* (cDEP) and *traveling-wave DEP* (twDEP). The former arises from a spatially varying *magnitude* of the field while the latter is due to its spatially varying *phase*. The closely related concepts of *electro-orientation* and *electrorotation*, both causing a torque acting on the object, are usually treated separately in the literature. A shared name—*generalized DEP* (gDEP), coined in Ref. [2]—can be used to jointly describe all the above-mentioned polarization-related phenomena. The review of gDEP may be found, for example, in Ref. [3], where the authors consider not only the quasistatic but also arbitrary time-varying fields. The latter is denoted as the *transient gDEP* or the *polarization history* (or *crossing trajectory*) effect. However, since the period of the ac electric field is usually much higher than the timescale related to the object's movement, the quasistatic theory and related mathematical models are typically sufficient. Other useful resources concerning DEP are, for example, Refs. [4–7].

A mathematical model of DEP enables us not only to perform various simulations and analyses helping us to understand the described physics but is also necessary when it comes to applying DEP to a precise position and orientation control of the micro-objects. In such cases, apart from the model accuracy, also its computational time becomes essential as it is detailed in Ref. [8], where we described a device for independent position control of several microspheres. Following this motivation, we aim at developing a real-time evaluable model for DEP force and torque computation applicable not only to spherical but to arbitrarily shaped objects.

*tomas.michalek@fel.cvut.cz; http://aa4cc.dce.fel.cvut.cz/
†aude.bolopion@femto-st.fr

A. State of the art

There are two basic approaches for modeling DEP: the *Maxwell stress tensor* (MST) method [9] and the *effective moments* (EM) method [2,10–13]. The former is considered the most accurate, but since it is based on finite-element-method (FEM) computations, it imposes huge time and memory requirements. The latter method is, on the other hand, just an approximation of the actual DEP force and torque, but it leads to analytical formulas for force and torque computations, and thus it is fast to evaluate. The key idea here is that the electric field of a polarized object is represented by a set of electric multipoles of an increasing order (the higher the order of the multipole, the higher the accuracy of the approximation) and the total DEP force and torque is then the sum of the forces and torques acting on these individual multipoles. The accuracy of the EM method under various scenarios and using various orders of approximation was investigated, for example, in Refs. [14–16] and in Ref. [17]. Generally, the higher-order multipolar moments are necessary for situations when the external polarizing electric field is highly inhomogeneous or when the object is of some complicated shaped. In practice, however, the use of this method is so far essentially limited to spherical objects only. That is because only for them can a multipolar description for general harmonic electric fields be obtained. Partial results exist for ellipsoidal objects [18,19], for which analytical formulas for induced dipole are known, and also for any other cylindrically symmetrical objects [20,21], for which multipolar moments up to the ninth order can be obtained from numerical simulations. In both of these cases, the symmetry requirement stems from the fact that only the linear multipoles (all the charges are constrained to a single line) are used for the description of the polarized object. Moreover, this also means that these methods are only valid if the external electric field is rotationally symmetric along the symmetry axis of the object.

B. Contribution

We propose a method for online (in real time) computation of multipolar moments describing the electric field of an arbitrarily shaped polarized object that does not pose any limitations regarding the shape, material properties, or even inhomogeneity of the object. Its orientation in space or the external polarizing electric field itself can also be arbitrary. The obtained multipoles can then be used in the EM method, which significantly extends its practical applicability. The resulting real-time evaluable model can serve as a solid foundation for a future design of control algorithms achieving simultaneous DEP-based position and orientation control of arbitrarily shaped micro-objects in fluidic media.

In this paper, we consider that the object of interest is located in a quiescent fluid sufficiently far from any other objects or obstacles. Modeling of the interaction between more nonspherical objects is a subject of future research, as is the modeling of the hydrodynamic effects influencing the object's motion in a fluid.

II. PROPOSED MODELING SCHEME

The proposed method extends the use of the EM method and deals with its essential elements—the multipolar moments—and hence we will start by summarizing basic existing concepts.

A. Multipolar moments and EM method

In the EM method, multipolar moments (or multipoles) are used to describe a potential due to a charge distribution inside a polarized object. As will be shown below, such a description is, however, only approximate.

1. Multipolar moments

Consider an arbitrary external electrostatic source field in an empty space described by an associated electric potential Φ_{empty}. If we place an electrically neutral (uncharged) object of interest into this field, then the object polarizes and the potential field changes to Φ_{filled}. It holds that $\Phi_{\text{filled}} = \Phi_{\text{empty}} + \Phi_{\text{object}}$, where Φ_{object} is the potential corresponding to the newly emerged charge distribution inside the object due to its polarization. We will denote the mentioned charge distribution by $\rho(\boldsymbol{r})$. The object and thus also the whole charge distribution is, without the loss of generality, confined to an interior of a virtual sphere S of radius R located at the origin of the coordinate system. Outside this sphere the potential there can be written as the volumetric integral

$$\Phi_{\text{object}}(\boldsymbol{r}) = \frac{1}{4\pi\epsilon_f}\int_{S(R)} \frac{\rho(\boldsymbol{r})}{|\boldsymbol{r}-\boldsymbol{r}'|} d^3r', \quad \boldsymbol{r} \geqslant R, \tag{1}$$

where ϵ_f is the absolute permittivity of the surrounding fluidic medium, and $\boldsymbol{r}$ is a vector representing a position in space. By expanding the term $\frac{1}{|\boldsymbol{r}-\boldsymbol{r}'|}$ in Eq. (1) in a Taylor series about the origin, we get an infinite sum describing the potential using multipolar moments. Depending on whether we perform the expansion in Cartesian or spherical coordinates, we get *Cartesian multipolar moments* or *spherical multipolar moments*, both of which will be, due to their unique properties, useful in the following development. For the Cartesian case, we get

$$\Phi_{\text{object}}(\boldsymbol{r}) = \frac{1}{4\pi\epsilon_f}\left[\frac{\boldsymbol{p}^{(0)}}{r} + \frac{\boldsymbol{p}^{(1)}\cdot\boldsymbol{r}}{r^3} + \frac{1}{2}\sum_{i,j=1}^{3}\frac{r_i r_j}{r^5}p_{ij}^{(2)} + \cdots\right], \quad \boldsymbol{r} \geqslant R, \tag{2}$$

where $r = \|\boldsymbol{r}\|_2$, r_i is the ith element of vector $\boldsymbol{r}$, and $\boldsymbol{p}^{(n)}$ are the multipolar moments. For $n = 1$, we call the corresponding moment dipole, and for $n = 2$, we call it quadrupole, followed by octopole, hexadecapole, and 2^n-poles for even higher values of n. These are tensor quantities of the corresponding order, and the subscripts of p then refer to the individual elements of these tensors. Notice that the higher the order of multipole, the faster the decay of the corresponding term to zero with the increasing distance r from the origin. Depending on the required accuracy of the electric potential representation, we can trim the series in the brackets and use just the first few terms.

Similarly, when we perform the Taylor-series expansion in the case of spherical coordinates we get

$$\Phi_{\text{object}}(\boldsymbol{r}) = \frac{1}{\epsilon_f}\sum_{l=0}^{\infty}\sum_{m=-l}^{l}\frac{q^*_{l,m}}{2l+1}\frac{Y_{l,m}(\theta,\phi)}{r^{l+1}}, \tag{3}$$

where $q_{l,m}$ are the components of the multipolar moments in their spherical form. The subscript l determines the order of the moment, and $m = -l, \ldots, l$ denote its individual elements (but now the moment itself does not have a form of a tensor). The symbol $(\cdot)^*$ denotes a complex conjugate, $Y_{l,m}(\theta,\phi) = \sqrt{\frac{(2l+1)(l-m)!}{4\pi(l+m)!}}P_{l,m}(\cos\theta)e^{jm\phi}$ are so-called spherical harmonics defined using Legendre polynomials $P_{l,m}(\cos\theta)$, and, finally, $j = \sqrt{-1}$ is the imaginary unit.

Although the spherical form of multipolar moments clearly varies from the Cartesian one, they both represent the same quantity. By comparing the two expansions in Eqs. (2) and (3), it is possible to find expressions for mutual conversion between the two formulations (as was done, for example, in Ref. [22]). We will exploit the possibility to switch back and forth between these two descriptions in the paper.

2. EM method

Now we will show how to use the multipolar moments together with the EM method for computation of the DEP force and torque acting on any polarized object placed in an inhomogeneous external electric field. Since, as was already stated in the Introduction, harmonic fields of a sufficiently high frequency are used to avoid other unwanted electrokinetic effects, a time-averaged (over one period of a harmonic external electric field) force, $\langle\mathbf{F}\rangle$, and torque, $\langle\mathbf{T}\rangle$, are necessary to consider. They are given by the following formulas derived by Jones and Washizu in Ref. [12]:

$$\langle\mathbf{F}\rangle = \sum_{n=1}^{N}\langle\mathbf{F}^{(n)}\rangle = \sum_{n=1}^{N}\frac{1}{2}\text{Re}\left[\frac{\tilde{\boldsymbol{p}}^{(n)}[\cdot]^n\nabla^n\tilde{\mathbf{E}}^*}{n!}\right], \tag{4}$$

$$\begin{aligned}\langle\mathbf{T}\rangle &= \sum_{n=1}^{N}\langle\mathbf{T}^{(n)}\rangle \\ &= \sum_{n=1}^{N}\frac{1}{2}\text{Re}\left[\frac{1}{(n-1)!}(\tilde{\boldsymbol{p}}^{(n)}[\cdot]^{n-1}\nabla^{n-1})\times\tilde{\mathbf{E}}^*\right],\end{aligned} \tag{5}$$

where N is the order of approximation; $\mathbf{F}^{(n)}$ and $\mathbf{T}^{(n)}$ are the force and torque contributions, respectively, caused by a multipole of order n; $\langle\cdot\rangle$ denotes the time average; Re$[\cdot]$ is the real part of the expression; and ∇ is the gradient operator; the dyadic operation $[\cdot]^n$ stands for n dot multiplications and $\tilde{(\cdot)}$ is used to represent a phasor. Since only harmonic driving signals (electric fields or, actually, voltages) are considered, we can compactly represent the related quantities using a phasor notation encoding both their amplitude and phase.

Notice that the only quantities we need to know in order to compute the force and torque are the external harmonic electric field $\tilde{\mathbf{E}}$ and the multipolar moments of the polarized object in their Cartesian form $\tilde{\boldsymbol{p}}^{(n)}$. While computation of the electric field is tractable even online (in real time, see Sec. II F), the computation of general multipolar moments even in the offline regime is so far only available for spherical objects. In the following section we will first show how these moments can be obtained offline using numerical FEM simulations, and then we will explain how to use the same approach in a computational scheme achieving real-time performance. This will enable us to compute the DEP force and torque Eqs. (4) and (5) acting on an arbitrarily shaped and oriented object in an arbitrary external electric field in real time.

B. Numerical computation of multipolar moments for arbitrarily shaped objects

In the development, we will use the spherical form of multipoles here, because we will advantageously use their orthogonality property. The result can then be always translated to the Cartesian form as explained in the previous section. We will start with Eq. (3) for potential, which we will invert and express the individual multipolar moments $q_{l,m}$ as functions of the potential Φ_{object}. This potential field can be obtained by subtracting two numerical simulations $\Phi_{\text{filled}} - \Phi_{\text{empty}}$.

For further development the following property of spherical harmonics:

$$\oint_{S(R)} Y_{l,m}(\theta,\phi)Y^*_{l',m'}(\theta,\phi)d\Omega = R^2\delta_{ll'}\delta_{mm'}, \tag{6}$$

which stems from their orthonormality, is of particular importance. In the expression above, δ_{ij} is the Kronecker δ and $d\Omega = \sin\theta d\theta d\phi$, since the integration is over a unit sphere. Other two useful properties are the following conjugation rules for spherical harmonics and spherical multipolar moments:

$$q^*_{l,m} = (-1)^m q_{l,-m} \quad \text{and} \quad Y_{l,-m} = (-1)^m Y^*_{l,m}. \tag{7}$$

At first, let us apply the first conjugation rule from Eq. (7) to the potential expression in Eq. (3). We get

$$\Phi_{\text{object}}(\boldsymbol{r}) = \frac{1}{\epsilon_f}\sum_{l=0}^{\infty}\sum_{m=-l}^{l}\frac{(-1)^m q_{l,-m}}{2l+1}\frac{Y_{l,m}(\theta,\phi)}{r^{l+1}}. \tag{8}$$

Next we change the order of summation and apply the second conjugation rule from Eq. (7). We then multiply both sides of the equation by $Y_{l',m'}(\theta,\phi)$ and perform the integration over a sphere $S(R)$ [recall that $S(R)$ is a virtual sphere encapsulating the object of interest]. Here l' and m' are just auxiliary indices used to represent some specific spherical harmonic function. We obtain

$$\begin{aligned}&\oint_{S(R)}\Phi_{\text{object}}(\boldsymbol{r})Y_{l',m'}(\theta,\phi)dS \\ &= \oint_{S(R)}\frac{1}{\epsilon_f}\sum_{l=0}^{\infty}\sum_{m=-l}^{l}\frac{q_{l,m}}{2l+1}\frac{Y^*_{l,m}(\theta,\phi)}{r^{l+1}}Y_{l',m'}(\theta,\phi)dS.\end{aligned} \tag{9}$$

Most of the terms on the right-hand side are independent on the integration variable, and thus they can be factored out in front of the integral. Thanks to Eq. (6), almost all of the summands vanish. The only one remaining is the one for $l = l'$, $m = m'$, which enables us to express the associated

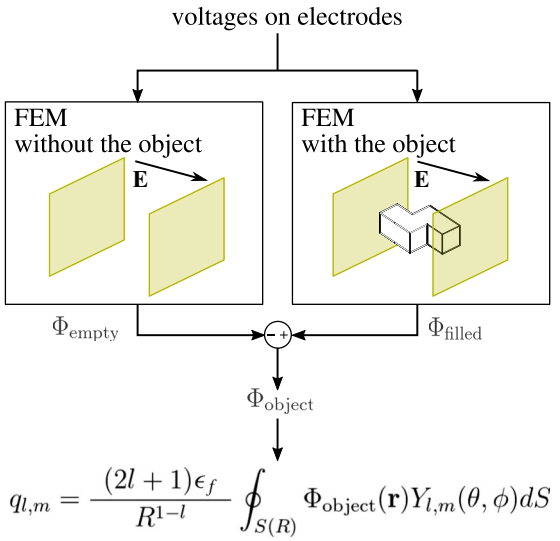

FIG. 1. Illustration of the procedure for extracting the spherical multipolar moments $q_{l,m}$ of arbitrary order for objects having an arbitrary shape. Here a Tetris "S" or "Z"-shaped object placed between two planar electrodes generating the external electric field is used as an example.

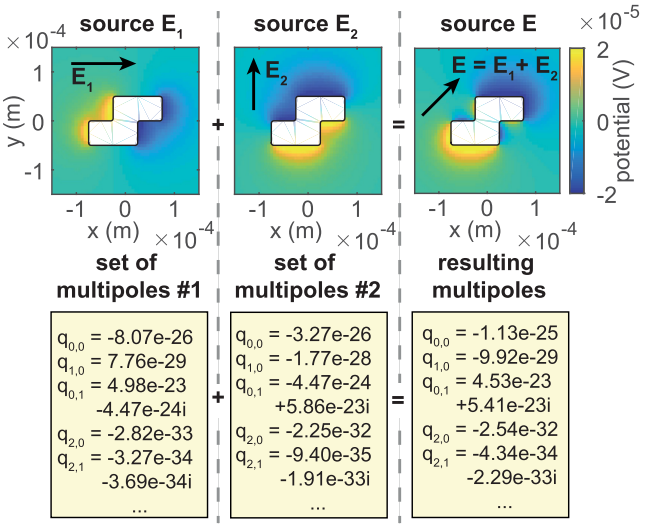

FIG. 2. Illustration of the superposition principle. Here the three uniform fields are $\mathbf{E}_1 = (1,0,0)^T$ V/m, $\mathbf{E}_2 = (0,1,0)^T$ V/m, and $\mathbf{E} = (1,1,0)^T$ V/m. We provide a complete list of all computed spherical multipoles together with their Cartesian equivalents in the Supplemental Material [23].

multipolar moment as

$$q_{l',m'} = \frac{(2l'+1)\epsilon_f}{R^{1-l'}} \oint_{S(R)} \Phi_{\text{object}}(\boldsymbol{r}) Y_{l',m'}(\theta,\phi) dS. \quad (10)$$

Indices l' and m' can now be switched back to l and m, respectively, to match the original notation,

$$q_{l,m} = \frac{(2l+1)\epsilon_f}{R^{1-l}} \oint_{S(R)} \Phi_{\text{object}}(\boldsymbol{r}) Y_{l,m}(\theta,\phi) dS. \quad (11)$$

All we need to know to evaluate Eq. (11) and thus to compute the multipolar representation of the object is a potential Φ_{object} on a surface of a virtual sphere $S(R)$ encapsulating it. It is interesting to note here that since we perform the integration over the surface of $S(R)$, Eq. (11) is kind of independent of the particular object's shape and it may seem that we are describing the polarization of the whole sphere instead of the polarization of the object itself. Indeed, the resulting multipolar moments describe the entire polarization-induced charge structure contained in $S(R)$, which may even go slightly beyond the boundaries of the object itself, but this is precisely the quantity of interest for the DEP force and torque computation.

Figure 1 summarizes the procedure for obtaining multipolar representation of an arbitrarily shaped and oriented object located in an arbitrary electric field including the calculation of Φ_{object} using the two FEM numerical simulations. As already noted above, the size of the sphere $S(R)$ is chosen to incorporate just the very charge structure resulting from the polarization of the object of interest. In our implementation, we make R around 1% bigger than is the half of the longest dimension of the object. This ensures that we capture the majority of the polarization-induced charge and also, depending on the particular implementation details, it can facilitate the meshing of the FEM model. In the following sections, we will show how to make this process real-time.

C. Superposition as the key principle

The problem of the previously described method is that every time the Φ_{object} changes, two time-consuming FEM simulations have to be carried out. This happens when the voltages on electrodes or the position of the object or its orientation changes, because then also the external electric field with respect to the object of interest changes (in fact, this is the only thing that matters).

A solution to this problem is to utilize the principle of superposition holding for an electric potential and as a consequence also for the multipolar moments [it can be seen, for example, from Eq. (11)]. As Fig. 2 illustrates, we can obtain a multipolar representation of the object polarized by a sum $\mathbf{E}_1 + \mathbf{E}_2$ of two different electric fields as a sum of multipolar moments generated by each of these fields separately. In this example a sum of two homogeneous electric fields is used for simplicity, but in general the same principle holds also for any linear combination of any number of even inhomogeneous electric fields and the corresponding multipolar descriptions they generate.

If we, in advance, compute and store the multipolar representation for a set of external fields forming a basis of all the possible source fields (instead just for $\mathbf{E}_1$ and $\mathbf{E}_2$), we can then get the multipoles associated to an arbitrary external field just in time necessary for computation of a linear combination.

The basic idea is therefore at first to run a set of offline computations to construct a *basis table of solutions* containing couples of *external electric field basis elements* and the *multipolar representations* of the object polarized by such field. Afterward, the principle of superposition could be used for online (real-time) computation, in which just the rows of the precomputed table are combined. The technicalities of this key idea will be further detailed below starting with the choice of the basis elements for the source electric field.

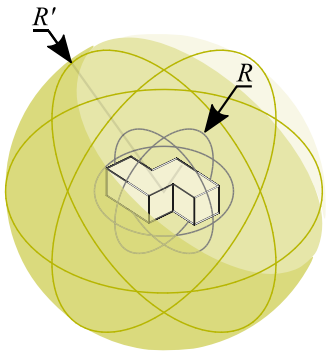

FIG. 3. Geometry used in the FEM solver. The larger sphere S' with a radius R' is used for setting the potential boundary conditions determining the source polarizing electric field. The smaller sphere S with a radius R defines a virtual surface over which we integrate in Eq. (11).

D. Basis of the source electric field

In this section, we will introduce two distinct but equivalent methods, in which the source electric field polarizing the object of interest can be described. Similarly to the case of multipolar moments, each of these formulations will be advantageous in different situations. We will also show how to convert back and forth between them.

One way to derive a basis, through which we can describe the source electric field polarizing the object of interest, is to start off with a Taylor series expansion of the electric field around the center position of the object. The values of spatial derivatives of the field constituting the individual terms of the series can then be used as coordinates with respect to a basis composed of all the available unit spatial derivatives. The similarity to the multipolar description of potential is of course not coincidental here. If the field had to be described accurately, then an infinite basis would be needed. In practice, however, its approximation using a finite basis will be sufficient. Anyway, we have to chose and use some order n of approximation for force and torque computations using the EM method, and therefore it makes no sense to consider electric fields with nonzero spatial derivatives of the order higher than $n-1$ here—the polarization caused by such an electric field could not be represented by multipolar moments of orders only up to n anyway.

This representation is, however, not particularly well suited for defining the external electric field in numerical FEM simulations. Here the field has to be represented purely just by boundary potential conditions. Therefore we encapsulate the object of interest in a sphere S' with a radius $R' > R$ (see Fig. 3), whose surface will carry these boundary conditions defying the polarizing electric field in its interior. The greater the R', the more accurate the results of the numerical FEM simulation will be (because of the mitigation of boundary effects), but also the more time and memory demanding the computation. In our implementation we used $R' \approx 10R$. Using the above-specified construction, the description of an arbitrary source electric field translates into a description of an arbitrary potential on the surface of $S'(R')$, to which purpose we can use the Eq. (3) evaluated on the given spherical surface. Thanks to the orthogonality of spherical harmonics, each of the addends represent one of the mutually orthogonal basis elements with elements $q_{l,m}$ serving as the corresponding coordinates. Mutual orthogonality of potentials means also a mutual orthogonality of the corresponding source electric fields. Similarly to the first case, it is sufficient to use only the first n multipolar moments to represent the source electric field, since representing it more accurately would not give us any further benefit. To distinguish that these spherical multipolar moments do not represent the potential of a polarized object, but rather describe the *external* source electric field, we will use the superscript "E"—$q^E_{l,m}$s.

To derive the expression converting the first-mentioned representation into the second one, we will do a thought experiment. Consider that the sphere, whose surface is used to define our potential boundary conditions, is filled by an ideally polarizable material. Under such a condition, the external electric field should vanish inside the sphere, and the resulting potential on its surface should be therefore exactly opposite to the external source potential field—the one we want to describe. Obtaining the multipolar description of this hypothetical ideally polarized sphere (and switching the signs) would therefore give us the result. Since for a sphere there exists an analytical expression for multipoles, we can easily obtain moments describing the desired potential. We utilize a formula,

$$\boldsymbol{p}^{(n)} = \frac{4\pi\epsilon_f R'^{(2n+1)} n K^{(n)}}{(2n-1)!!}\boldsymbol{\nabla}^{(n-1)}\mathbf{E}, \tag{12}$$

from Ref. [12] and evaluate it for such a hypothetical case of ideal polarization. Polarizability of the sphere is determined by its material properties (electric permittivity and conductivity) contained in $K^{(n)}$, the so-called generalized Clausius-Mossotti factor defined, for example, in Ref. [13]. For the considered case of ideally polarizable sphere $K^{(n)} \to \frac{1}{n}$. We can therefore represent the potential on the sphere of interest using the multipolar moments

$$\boldsymbol{p}^{E,(n)} = -\frac{4\pi\epsilon_f R'^{(2n+1)}}{(2n-1)!!}\boldsymbol{\nabla}^{(n-1)}\mathbf{E}. \tag{13}$$

The minus sign is there to take into account the fact that the potential due to such polarization would be opposite to the original one as already noted above. The resulting Cartesian multipole can then be just converted to its spherical form giving us the final q^Es. Conversion in the opposite direction can be done analogously.

E. Offline computation—Constructing the basis table

In this section we will cover all the details and technicalities encountered during the basis table construction.

To generate the basis we have to compute the multipolar moments of the object when polarized by each individual basis element of the source electric field. In practice, we do this by taking individual rows of Table I defying the basis elements, fitting the corresponding q^Es into Eq. (3) and applying the resulting potential as the boundary condition on the surface of $S'(R')$ of the FEM simulations. Note that the monopole term $q^E_{0,0}$ is always equal to zero since we assume that the object is electrically neutral. Further note that there are no negative indices related to q^Es. The reason is to save

TABLE I. Inputs to the offline computation

	Multipolar moments						
Sim No.	$q^E_{0,0}$	$q^E_{1,0}$	$q^E_{1,1}$	$q^E_{2,0}$	$q^E_{2,1}$	$q^E_{2,2}$	$\cdots$
1	0	1	0	0	0	0	$\cdots$
2	0	0	1	0	0	0	$\cdots$
3	0	0	j	0	0	0	$\cdots$
4	0	0	0	1	0	0	$\cdots$
5	0	0	0	0	1	0	$\cdots$
6	0	0	0	0	j	0	$\cdots$
7	0	0	0	0	0	1	$\cdots$
8	0	0	0	0	0	j	$\cdots$
$\vdots$	$\vdots$	$\vdots$	$\vdots$	$\vdots$	$\vdots$	$\vdots$	$\ddots$

both computational time and storage space, as these can be determined by the above-stated conjugation rules [Eq. (7)]. Since spherical multipolar moments are in general complex quantities, we have to also take into account their imaginary parts as can be seen, for example, in the third, sixth, or eighth row of Table I. An exception here are the elements $q^E_{a,0}$, $a \in \mathbb{Z}$, which have the imaginary part always equal to zero [this can be seen again from the conjugation rules in Eq. (7)]. Having the boundary potential conditions set, we then always perform two simulations—one without the object and the other with it. Subtracting these two (according to Fig. 1) we get the potential $\tilde{\Phi}_{\text{object}}$ of the polarized object serving as an input for computation of the multipoles.

So far, we silently considered only electrostatic source fields and the corresponding real potential fields in Secs. II A and II C. Also the expression Eq. (11) accepts only real potentials. But as the tilde in $\tilde{\Phi}_{\text{object}}$ indicates, the potential of the polarized object is generally complex. Even if the potential boundary conditions applied to the sphere surface are purely real, the differences in the material properties of the object and its surrounding medium (specifically their electric conductivities and permittivities) can cause the shift in the field's phase. We have to therefore treat separately the real and imaginary parts of the potential—$\text{Re}[\tilde{\Phi}_{\text{object}}]$ and $\text{Im}[\tilde{\Phi}_{\text{object}}]$, respectively. The two corresponding sets of multipolar moments have to be kept separately during storage as well as during subsequent calculations. Four superscripts will be used to denote the specific elements $q^{abcd}_{l,m}$ of the precomputed basis table. The first three superscripts encode the external source electric field used in the simulation. A field that is given by $q^E_{l,m} = 0$ except for a case when $l = a$ and $m = b$. In such situation the corresponding element of multipolar moment, $q^E_{a,b}$, is equal to either real or imaginary unit based on whether the third superscript $c = r$ or $c = i$, respectively. The last superscript d then determines whether it is the real ($d = r$) or the imaginary ($d = i$) part of $\tilde{\Phi}_{\text{object}}$ which is considered. Following this notation, $q^{10ir}_{2,1}$ is, for example, the second element of the second-order spherical multipolar moment extracted from a simulation, in which the external source potential on $S'(R')$ was given by real part of Eq. (3) evaluated with $q_{1,0} = j$ and all the other $q_{l,m} = 0$ for $l \neq 1 \wedge m \neq 0$. The above is summarized in Fig. 4.

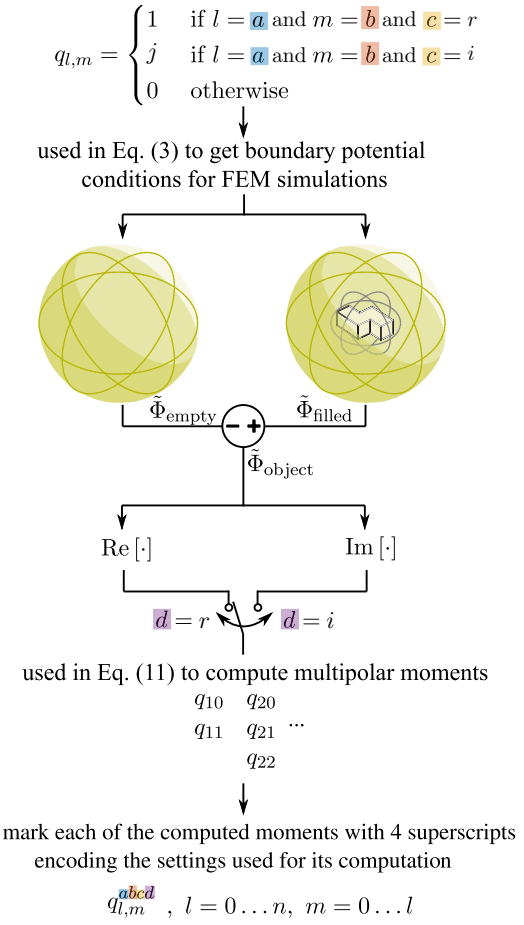

FIG. 4. Generating and denoting the basis elements.

From each simulation, we will therefore obtain $2(1 + 2 + \cdots + n) = n(n + 1)$ complex values—the elements of our basis table of solutions. We store them in a table alongside with the corresponding q^Es describing the source electric field. For illustration, please see Table II, where the reference to the source electric field is made through the specific simulation number.

TABLE II. Outputs from the offline computation

Sim No.	Stored data table					
1	$q^{10rr}_{1,0}$	$q^{10rr}_{1,1}$	$q^{10rr}_{2,0}$	$q^{10rr}_{2,1}$	$q^{10rr}_{2,2}$	$\cdots$
	$q^{10ri}_{1,0}$	$q^{10ri}_{1,1}$	$q^{10ri}_{2,0}$	$q^{10ri}_{2,1}$	$q^{10ri}_{2,2}$	$\cdots$
2	$q^{11rr}_{1,0}$	$q^{11rr}_{1,1}$	$q^{11rr}_{2,0}$	$q^{11rr}_{2,1}$	$q^{11rr}_{2,2}$	$\cdots$
	$q^{11ri}_{1,0}$	$q^{11ri}_{1,1}$	$q^{11ri}_{2,0}$	$q^{11ri}_{2,1}$	$q^{11ri}_{2,2}$	$\cdots$
3	$q^{11ir}_{1,0}$	$q^{11ir}_{1,1}$	$q^{11ir}_{2,0}$	$q^{11ir}_{2,1}$	$q^{11ir}_{2,2}$	$\cdots$
	$q^{11ii}_{1,0}$	$q^{11ii}_{1,1}$	$q^{11ii}_{2,0}$	$q^{11ii}_{2,1}$	$q^{11ii}_{2,2}$	$\cdots$
4	$q^{20rr}_{1,0}$	$q^{20rr}_{1,1}$	$q^{20rr}_{2,0}$	$q^{20rr}_{2,1}$	$q^{20rr}_{2,2}$	$\cdots$
	$q^{20ri}_{1,0}$	$q^{20ri}_{1,1}$	$q^{20ri}_{2,0}$	$q^{20ri}_{2,1}$	$q^{20ri}_{2,2}$	$\cdots$
$\vdots$	$\vdots$	$\vdots$	$\vdots$	$\vdots$	$\vdots$	$\ddots$

F. Computing the electric field

We generate the field typically by applying voltages on the set of microelectrodes (see, for example, our DEP systems [8,24]). Knowing the voltage signals applied to the electrodes, we can compute the electric field and its spatial derivatives (encoding also the field's inhomogeneity) at the object's location. In some specific cases of electrode designs an analytical solution may be known (for example, for the interdigitated electrode arrays [25,26]), and in others one has to settle for the numerical solution [24] or combined approaches [27,28].

Here we used an approximate method based on Green's functions similar to the one described in Ref. [27]. Its advantage is that it results in an analytical expression of potential, though only approximate and very complicated. Still, we can differentiate it and thus obtain higher spatial derivatives of the electric field than what could be possible with a FEM-based numerical solution. In contrast to the referred solution, we used a slightly different discretization scheme. Instead of using semi-infinite rectangles suitable for the specifically used electrode array, we divided the electrode plane into small-enough square bins enabling us to approximate arbitrary shapes of the electrodes. The same approach as in Refs. [8,24] using the lookup table for electric field and its derivatives was used to obtain the field in real time. These are then [using Eq. (13) and subsequent conversion to spherical form of multipoles] represented by $q^E_{l,m}$s for further use in the online computation.

G. Online computation—Doing the linear combination

Knowing the precomputed basis table of multipolar moments and the external electric field expressed using q^Es, we can obtain the resulting multipolar moments by a linear combination as mentioned in Sec. II C.

At first, let us for simplicity assume that the source electric field is just real. Even in this simplified case, we have to, when doing the linear combination, make sure that we combine always just the mutually corresponding elements of the source field and the basis,

$$q^{cr}_{l,m} = \sum_{l'=1}^{n}\sum_{m'=0}^{l'} \mathrm{Re}\big[q^E_{l',m'}\big] q^{l'm'cr}_{l,m}, \quad \text{where } c \in \{r,i\}, \tag{14}$$

$$q^{ci}_{l,m} = \sum_{l'=1}^{n}\sum_{m'=0}^{l'} \mathrm{Im}\big[q^E_{l',m'}\big] q^{l'm'ci}_{l,m}, \quad \text{where } c \in \{r,i\}. \tag{15}$$

This way we get for every l and m (denoting the specific lth element of the resulting multipolar moment of order m) four quantities: $q^{rr}_{l,m}$, $q^{ri}_{l,m}$, $q^{ir}_{l,m}$, and $q^{ii}_{l,m}$. Each of these spherical moments are then converted back to their Cartesian form ($q^{cd}_{n,0}, q^{cd}_{n,1}, \ldots q^{cd}_{n,n} \rightarrow \boldsymbol{p}^{(n),cd}$, where $c, d \in \{r,i\}$) and assembled the following way to just one final complex Cartesian moment:

$$\boldsymbol{p}^{(n)} = [\boldsymbol{p}^{(n),rr} + \boldsymbol{p}^{(n),ri}] + j[\boldsymbol{p}^{(n),ir} + \boldsymbol{p}^{(n),ii}]. \tag{16}$$

In this form, they can be finally used to compute the dielectrophoretic force and torque.

In a case when the source potential itself can be complex (e.g., when there are phase-shifted signals applied to the electrodes), we will have instead of just one set of linear combination coefficients, $q^E_{a0}, q^E_{a1}, \ldots, q^E_{aa}$, and two such sets, $q^{E,r}_{a0}, q^{E,r}_{a1}, \ldots, q^{E,r}_{aa}$ and $q^{E,i}_{a0}, q^{E,i}_{a1}, \ldots, q^{E,i}_{aa}$, representing the real and the imaginary parts of the external electric field, respectively. The linear combination of the basis elements then reads

$$q^{cdr}_{l,m} = \sum_{l'=1}^{n}\sum_{m'=0}^{l'} \mathrm{Re}\big[q^{E,c}_{l',m'}\big] q^{l'm'dr}_{l,m}, \quad c,d \in \{r,i\}, \tag{17}$$

$$q^{cdi}_{l,m} = \sum_{l'=1}^{n}\sum_{m'=0}^{l'} \mathrm{Im}\big[q^{E,c}_{l',m'}\big] q^{l'm'di}_{l,m}, \quad c,d \in \{r,i\}, \tag{18}$$

giving us for every l and m eight quantities: $q^{rrr}_{l,m}$, $q^{rri}_{l,m}$, $q^{rir}_{l,m}$, $q^{rii}_{l,m}$, $q^{irr}_{l,m}$, $q^{iri}_{l,m}$, $q^{iir}_{l,m}$, and $q^{iii}_{l,m}$. These are then again converted to their Cartesian form and combined together the following way:

$$\begin{aligned}\boldsymbol{p}^{(n)} = {} & \{[\boldsymbol{p}^{(n),rrr} + \boldsymbol{p}^{(n),rri}] + j[\boldsymbol{p}^{(n),rir} + \boldsymbol{p}^{(n),rii}]\} \\ & + j\{[\boldsymbol{p}^{(n),irr} + \boldsymbol{p}^{(n),iri}] + j[\boldsymbol{p}^{(n),iir} + \boldsymbol{p}^{(n),iii}]\}\end{aligned} \tag{19}$$

to get one resulting Cartesian moment suitable for DEP force and torque computations using Eq. (4) and Eq. (5).

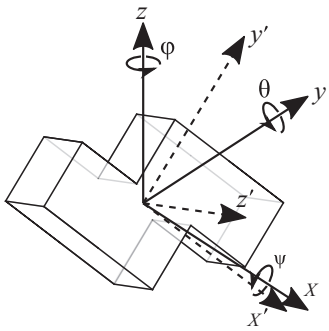

FIG. 5. Definition of the angles for rotation of the reference frame.

H. Considering orientation of the object

So far, we considered the orientation of the object to be fixed. In practice, however, the manipulated object can freely revolve in space and thus change its orientation as it moves through the medium. From the force and torque computation point of view, it is just the *relative* orientation of the object with respect to the field, which is important. Instead of rotating the object (leading to recomputation of the basis table), it is therefore better to express the electric field and its necessary spatial derivatives in a new rotated frame of reference, which is always attached to it as shown in Fig. 5. After performing the force and torque computation, the results have to be again translated back into the original global coordinate system. We do so by merely multiplying the resulting column vectors of forces and torques from left by a corresponding rotational matrix,

$$\mathbf{R} = \begin{bmatrix} \cos(\phi) & -\sin(\phi) & 0 \\ \sin(\phi) & \cos(\phi) & 0 \\ 0 & 0 & 1 \end{bmatrix} \begin{bmatrix} \cos(\theta) & 0 & \sin(\theta) \\ 0 & 1 & 0 \\ -\sin(\theta) & 0 & \cos(\theta) \end{bmatrix} \times \begin{bmatrix} 1 & 0 & 0 \\ 0 & \cos(\psi) & -\sin(\psi) \\ 0 & \sin(\psi) & \cos(\psi) \end{bmatrix}. \tag{20}$$

I. Summary

The above-described control-oriented model may be summarized using the pseudocodes in Algorithm 1 for the preprocessing procedure and in Algorithm 2 for the part of the model evaluated in real time.

Algorithm 1 Preprocessing steps (offline)

1: **for all** sets of multipolar moments given by rows of Table I **do**
2: load a FEM simulation model for an empty spherical domain
3: set the boundary potential condition on a surface of the sphere according to Eq. (3)
4: solve for the potential $\mathbf{\Phi}_{\text{empty}}$ inside a sphere
5: load a FEM simulation model for a spherical domain with an object of interest being placed inside it
6: set the boundary potential condition on a surface of the sphere according to Eq. (3)
7: solve for the potential $\mathbf{\Phi}_{\text{filled}}$ inside a sphere
8: compute $\mathbf{\Phi}_{\text{object}} = \mathbf{\Phi}_{\text{filled}} - \mathbf{\Phi}_{\text{empty}}$
9: extract the values of spherical multipolar moments using Eq. (11)
10: store the extracted moments alongside with the corresponding row of Table I (description of the source field) as for example shown in Table II
11: **end for**
12: define a dense enough grid of points in space in which we would like to compute DEP force and torque
13: **for all** of the electrodes **do**
14: **for all** points in the grid **do**
15: compute the electric field and its various spatial derivatives using the Green's function approach for a situation when a potential of 1 V is set to the specific electrode and the rest of them is kept grounded
16: **end for**
17: **end for**
18: store the results as a lookup table

Algorithm 2 Real-time evaluation steps (online)

1: compute the electric field derivatives at the point in space where the object is located (using interpolation in the precomputed look-up table and the principle of superposition)
2: get the Cartesian multipoles describing the potential on a virtual ideally polarizable sphere centered at the object's location (using expression Eq. (13))
3: convert them to spherical form of multipolar moments
4: use the results as the coefficients of the linear combination of the precomputed basis elements (see step 10 of Algorithm 1)
5: convert the resulting multipolar moments back into the Cartesian formulation
6: use the EM method to compute the DEP force and torque (Eq. (5))

III. RESULTS AND DISCUSSION

A Tetris "S" or "Z" piece depicted in Fig. 6 was used as an example of an object, for which the real-time force and torque computations were so far unavailable. The dimensions of the object are included in the picture.

At first, we will demonstrate the validity of the derived Eq. (11). Consider an object polarized by an uniform external

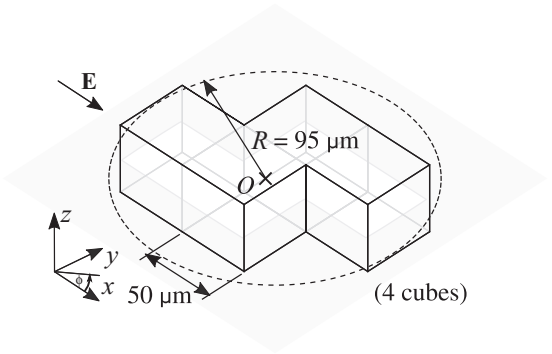

FIG. 6. Dimensions of the Tetris-shaped micro-object used in the example and validation simulations.

electric field with an intensity of 1 V/m pointing along the x axis. We use Eq. (11) to compute the multipolar representation of the object, and then we put the results back into Eq. (3) and compare the reconstructed potential against the solution obtained numerically using COMSOL MULTIPHYSICS 5.1. Figure 7 shows the results for various orders of approximation. The higher the order of multipoles, the more accurate the representation of the potential.

To prove the validity of the model as a whole, we compared its outcomes against the reference solutions obtained from COMSOL MULTIPHYSICS 5.1, where we performed time-independent computations of DEP forces and torques using MST method. As a test scenario, we used the so-called quadrupolar electrode array, which is usually used for torque generation in electrorotation experiments, but it can equally easily generate a DEP force. It is shown together with all the relevant dimensions in Fig. 8. As the driving signals, we used four sinusoidal waveforms having amplitudes 10, 10, 50, and 50 V, respectively, and phase shifts 0°, 90°, 180°, and 270°, respectively. The object's orientation was set such that from its initial orientation (as depicted in Fig. 8) it was rotated by 45° and 25° subsequently about the x and y axes. Its geometric center was placed on the z axis. DEP forces and torques were then computed for values of z ranging from from 60 to 150 μm. To keep the errors negligible, we used moments up to the fifth order

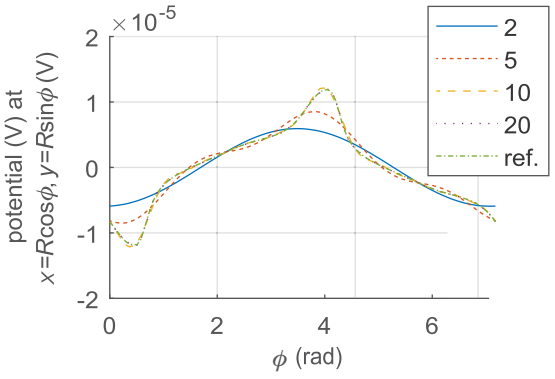

FIG. 7. Comparison of potentials along the circle laying in the xy plane and enclosing the object as depicted in Fig. 6 for various orders of approximation.

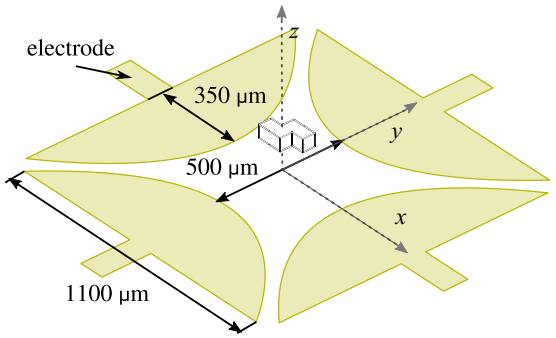

FIG. 8. Dimensions of the electrode array and Tetris-shaped micro-object used in the validation simulations.

(32-poles). Note that to accurately represent polarization of nonspherical objects, the higher-order multipolar moments will be necessary even when the external electric field is uniform as could be already seen in the potential comparison shown in Fig. 7.

The results plotted in Figs. 9 and 10 show that our model resembles well the reference solution when high-enough order of multipoles is used. At lower z coordinates, when the object is close to the edges of the electrodes, the electric field around the object becomes more inhomogeneous. Consequently, the accuracy of the solution gets worse. Surprisingly, the higher-order multipoles do not improve the accuracy of solution in this region. This is in contrast with the cases of higher z coordinates, where the accuracy does improve with increasing order of the multipole. We suspect that the reason for this is a not accurate enough computation of the electric field and especially its higher-order spatial derivatives near the electrodes. Since the method of Green's function, which we use for computation of the external electric field, uses just an approximation of the potential boundary conditions on the electrodes, it cannot provide accurate enough results in their vicinity.

TABLE III. Comparison of the computational times of different models of DEP forces and torques.

Model		Computational time
EM method	$n = 1$ (dipole)	0.1 ms
	$n = 2$ (quadrupole)	0.2 ms
	$n = 3$ (octopole)	0.6 ms
	$n = 4$ (hexadecapole)	2.1 ms
	$n = 5$ (32-pole)	9.3 ms
Maxwell stress tensor method		1 h 40 m 57 s

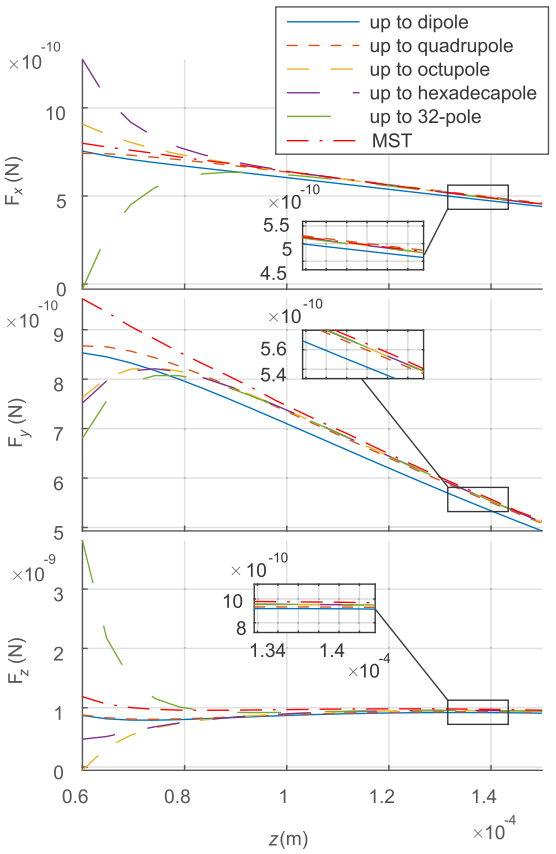

FIG. 9. Comparison of the force prediction obtained by the described model and the reference MST model.

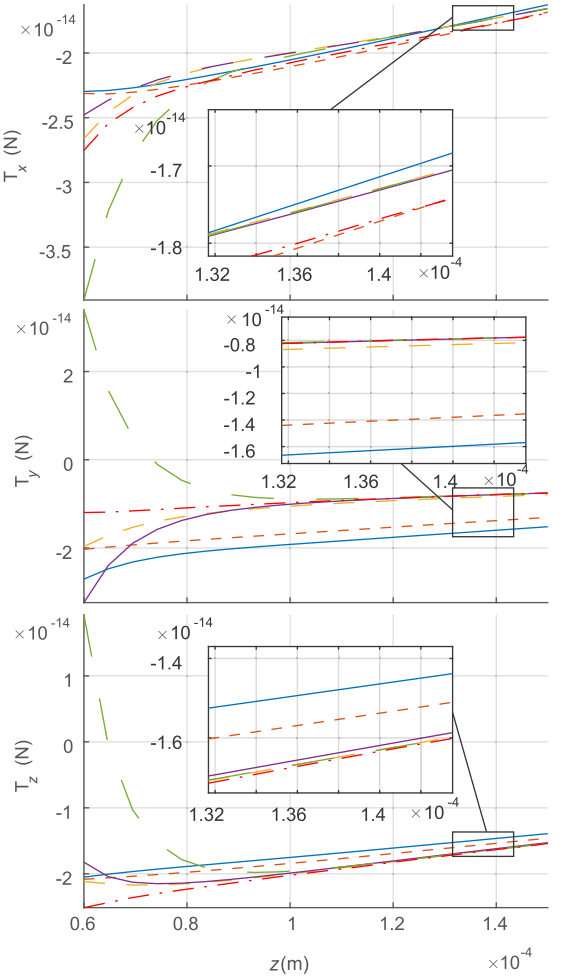

FIG. 10. Comparison of the torque prediction obtained by the described model and the reference MST model.

During the simulations made above, we measured the times required for computation of DEP forces and torques by both the MST method and our proposed model. A conventional PC (Intel Core i5, 3.30 GHz, 8 GB RAM, 64-bit, Win 7) was used. The results for different orders of approximation are stated in Table III. The evaluation of our model is much faster than performing the numerical simulation for the MST method. Nevertheless, with the increasing number of multipoles, the computational time t (in seconds) rises exponentially approximately according to $t = (9.768 \times 10^{-6})e^{1.37n}$, which means that the highest possible multipole computable under the time limit of 1 s would in the current implementation be the 256-pole ($n = 8$).

Since all the necessary numerical simulations can be done in advance (and just once for every new shape of the object), the real-time evaluation of the model takes only fractions of a second in comparison with hours of MST computation. Our MATLAB implementation of the described mathematical model can be found at [29].

IV. CONCLUSION

We introduced a simulation scheme based on EM method capable of real-time computation of the DEP forces and torques acting on objects of arbitrary shapes under arbitrary orientations and located in arbitrary electric fields. The enabling ingredient is the use of numerical solutions of the Laplace equation for getting the multipolar description of objects under such general scenarios. A specific way of how to construct a solution basis (from precomputed solutions) is then described so that all further computations can be done in real time. As such, the described control-oriented model could be used in future for simultaneous control of position and orientation of nonspherical objects with the envisioned biology and microassembly applications.

ACKNOWLEDGMENTS

This work has been supported by the EIPHI Graduate School (Contract No. ANR-17-EURE-0002), by the French RENATECH network and its FEMTO-ST technological facility, by the ANR and FNS project CoDiCell (Grant No. ANR-17-CE33- 0009), by the MiMedi project funded by BPI France (Grant No. DOS0060162/00) and the European Union through the European Regional Development Fund of the Region Bourgogne- Franche-Comte (Grant No. FC0013440), and by the Czech Science Foundation within the project P206/12/G014 (Center for Advanced Bioanalytical Technology, http://www.biocentex.cz).

[1] H. A. Pohl, *Dielectrophoresis: The Behavior of Neutral Matter in Nonuniform Electric Fields* (Cambridge University Press, Cambridge, 1978).
[2] X.-B. Wang, Y. Huang, F. F. Becker, and P. R. C. Gascoyne, J. Phys. D: Appl. Phys. **27**, 1571 (1994).
[3] U. Lei and Y. J. Lo, IET Nanobiotechnol. **5**, 86 (2011).
[4] T. B. Jones, *Electromechanics of Particles* (Cambridge University Press, Cambridge, 2005).
[5] H. Morgan and N. G. Green, *AC Electrokinetic: Colloids and Nanoparticles*, 1st ed. (Research Studies Pr, Philadelphia, PA, 2002).
[6] M. P. Hughes, *Nanoelectromechanics in Engineering and Biology* (CRC Press, Boca Raton, FL, 2002).
[7] R. R. Pethig, *Dielectrophoresis: Theory, Methodology and Biological Applications*, 1st ed. (Wiley, Hoboken, NJ, 2017).
[8] J. Zemánek, T. Michálek, and Z. Hurák, Electrophoresis **36**, 1451 (2015).
[9] X. Wang, X.-B. Wang, and P. R. C. Gascoyne, J. Electrost. **39**, 277 (1997).
[10] T. B. Jones, J. Electrost. **6**, 69 (1979).
[11] M. Washizu and T. B. Jones, J. Electrost. **33**, 187 (1994).
[12] T. B. Jones and M. Washizu, J. Electrost. **37**, 121 (1996).
[13] T. B. Jones, IEEE Eng. Med. Biol. Mag. **22**, 33 (2003).
[14] A. M. Benselama, É. Canot, and P. Pham, TechConnect Briefs **1**, 188 (2004).
[15] C. Rosales and K. M. Lim, Electrophoresis **26**, 2057 (2005).
[16] H. Nili and N. G. Green, Phys. Rev. E **89**, 063302 (2014).
[17] T. Michálek and J. Zemánek, Electrophoresis **38**, 1419 (2017).
[18] J. A. Stratton, *Electromagnetic Theory* (John Wiley & Sons, New York, 2007).
[19] C. Y. Yang and U. Lei, Appl. Phys. Lett. **90**, 153901 (2007).
[20] N. G. Green and T. B. Jones, J. Phys. D: Appl. Phys. **40**, 78 (2007).
[21] A. Ogbi, L. Nicolas, R. Perrussel, S. J. Salon, and D. Voyer, IEEE Trans. Magn. **48**, 675 (2012).
[22] J. D. Jackson, *Classical Electrodynamics*, 3rd ed. (Wiley, New York, 1998), Chap. 4, p. 146.
[23] See Supplemental Material at http://link.aps.org/supplemental/10.1103/PhysRevE.99.053307 for a complete list of multipolar moments related to example in Fig. 2.
[24] J. Zemánek, T. Michálek, and Z. Hurák, Lab on a Chip **18**, 1793 (2018).
[25] T. Sun, H. Morgan, and N. G. Green, Phys. Rev. E **76**, 046610 (2007).
[26] D. E. Chang, S. Loire, and I. Mezić, J. Phys. D: Appl. Phys. **36**, 3073 (2003).
[27] M. Gurtner, K. Hengster-Movric, and Z. Hurák, J. Appl. Phys. **122**, 054903 (2017).
[28] V. Gauthier, A. Bolopion, and M. Gauthier, Micromachines **8**, 253 (2017).
[29] T. Michálek, computer code, available at https://github.com/michato4/dep_model, Czech Technical University in Prague, Prague, 2018.